The on-state of single-crystal and polycrystalline NbO_2

Gary C. Vezzoli and L. W. Doremus
U.S. Army Armament Research and Development Command, Applied Sciences Division, Dover, New Jersey 07801

Steve Levy and G. K. Gaulé
U.S. Army Electronics Techology and Devices Laboratory, Fort Monmouth, New Jersey 07703

B. Lalevic and M. Shoga
Electrical Engineering Deparment, Rutgers University, P. O. Box 909, Piscataway, New Jersey 08854

(Received 24 March 1980; accepted for publication 29 July 1980)

Single-crystal and polycrystalline NbO_2 switching devices were studied by double pulse and pulse interruption techniques. Results for single-crystal devices indicated a recovery time of 0.8–1.2 μs that is independent of the polarity relationship of the first and second switching pulses. Voltage interruptions, obtained by pulses of variable duration in opposition to the on-voltage, provided excursions into the on-state and revealed plateau regions in device voltage versus time. Hence the opposition or "diagnostic" pulse provides a region of rapidly decreasing on-state voltage followed by a region of zero on-voltage, from which current-voltage (I-V) data can be measured. An I-V curve of the on-state, thus obtained, showed a transitional region from an Ohmic state to a lower conductance subregime (of on-state). Below the holding voltage the time required to develop this lower-conductance subregime is about 50 ns for a single-crystal device, agreeing favorably with results from cw studies. The related time interval for polycrystalline devices is 250–350 ns. The interval between the holding voltage and the beginning of the transitional regime (10–20 ns) is interpreted to be the trapped carrier lifetime or emission time.

PACS numbers: 72.20.Ht. 85.30.De

I. INTRODUCTION

Reversible threshold switching from a high- to a low-resistance state is clearly established in single-crystal and polycrystalline NbO_2.[1–5] Fast response (1 ns), high off-state resistance (~ 1 MΩ), and low off-state capacitance (< 10 pF) are properties of NbO_2 devices which satisfy requirements for applications as protectors or surge arrestors in rf receivers. Reproducibility of switching parameters and device lifetime were considerably improved by deposition of bismuth electrodes on the NbO_2 active material.[6] A nonthermal mechanism for the threshold switching in NbO_2 (Ref. 5) is strongly supported by the on-state I-V data and recovery curve data.

In earlier works[4,7] studying the recovery behavior of the on-state of polycrystalline NbO_2 it was found that the on-state could survive for 200–400 ns (τ_2) at zero on-voltage without the requirement of a subsequent partial switching event to reinitiate the on-state. Continuous square and triangular wave (cw) studies of the on-state I-V characteristics indicated a higher-conductance Ohmic region as well as a lower-conductance linear and superlinear subregime beneath a charcteristic knee level.[4] From data on the required frequency and amplitude to dynamically sustain the on-state of polycrystalline devices of filament geometry given in Ref. 5, it was concluded that at least 5×10^9 electrons undergo recombination in an interruption time of about 200 ns. It was also shown in the previous studies,[4,7] that a voltage fall-time of about 100–150 ns was the maximum allowable time such that the on-state would be preserved without decay.

The purpose of the present work is to explore the on-state I-V characteristics of single-crystal NbO_2 devices during and subsequent to very short interruptions at zero voltage. These characteristics include the determination of the recovery time and the subholding-voltage time necessary to develop the subregime of lower conductance.

II. EXPERIMENTAL PROCEDURE

Single crystals of NbO_2 were produced by the Czochralsky-Kypopoulos technique in a triarc furnace and in an argon atmosphere. Crystals were subsequently sliced into thin wafers, 40–50 μm thick and 2–3 mm in diameter. Wafers were etched in an ammonium bifluoride (NH_4FHF) solution at 100 °C, then cleaned in an ultrasonic bath with propanol, and then, for the thinner and more fragile specimens, further cleaned with deionized water in a gelatine medium. Electrodes were vapor deposited in a vacuum of 10^{-6} Torr. Top electrodes consisted of three metallic layers: a 1000-Å Bi film vapor deposited first onto NbO_2, then 20 Å of Cr, and finally 500 Å gold. The lower electrode (0.87 mm^2) consisted of a 500-Å gold film. The final device configuration was thus Au-Cr-Bi-NbO_2-Au, with Au wires thermally bonded to the electrodes. The deposition of the thin Cr film increased the adhesion of Au film to the wafer, and thus facilitated the bonding process. The single-crystal device was finally encapsulated in a MODPAK unit with coaxial line. Between experiments the device was stored in a vacuum dessicator. Polycrystalline devices were fabricated using procedures described in Refs. 1–5, but with the electrode configuration cited above.

Electrical measurements were performed on the single-crystal samples using the circuit given in Fig. 1(a), and polycrystalline samples were addressed using the circuit shown

 0021-8979/81/020833-07$01.10

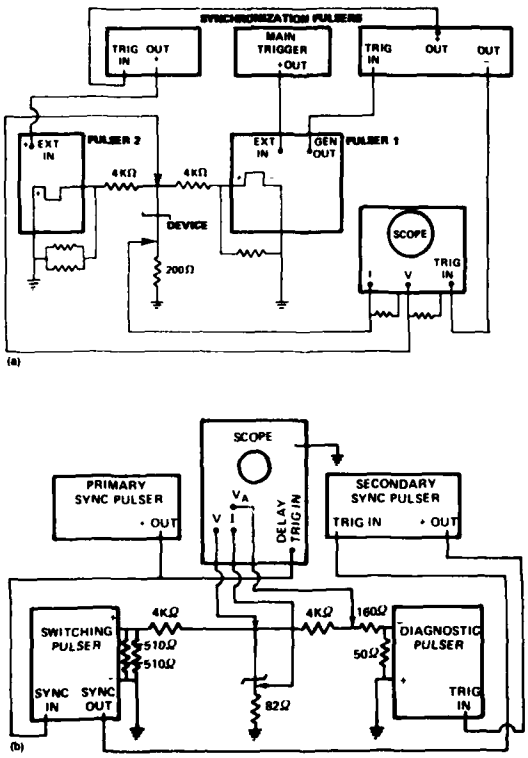

FIG. 1. Circuit diagram for diagnostic probing and double pulse experiments of NbO_2 on-state; (a) single crystal and (b) polycrystalline.

in Fig. 1(b). In both cases care was taken to eliminate noise and parasitic effects to be assured that the voltages and currents obtained on a Tektronix 7834 memory oscilloscope referred to device characteristics even at time scales as expanded as 2 ns/div. For the single-crystal studies the main and diagnostic pulsers were high power pulse generators (Cober model 605P), whereas for the polycrystalline devices a Hewlett-Packard model 214 A generator served as the diagnostic pulser. The essentially noise-free signals were achieved through the use of matching and balancing resistors, careful grounding procedures, and the use of an isolation transformer.

Typical single-crystal devices had a threshold voltage (V_{th}) of about 1300 V for set pulses of 3 μs duration. Off-state resistance ranged from 300 kΩ to 1 MΩ, and switching characteristics were quite reproducible from one set of experiments to another. Polycrsytalline devices showed a V_{th} generally ranging from 300 to 800 V depending upon sample thickness (10–15 μm) and were also reproducible and consistent in properties. However, a few thin samples (5–8 μm) exhibited lower V_{th} but approximately the same threshold field. The polycrystalline devices were normally not encapsulated and required the use of point contact pressure probes in conjunction with a manipulator device; hence some ringing developed owing to leads and contact effects.

Curve tracer data were taken after single pulse studies were completed, so as not to cause any thermal degradation due to 120-Hz extended operation. High-frequency (100

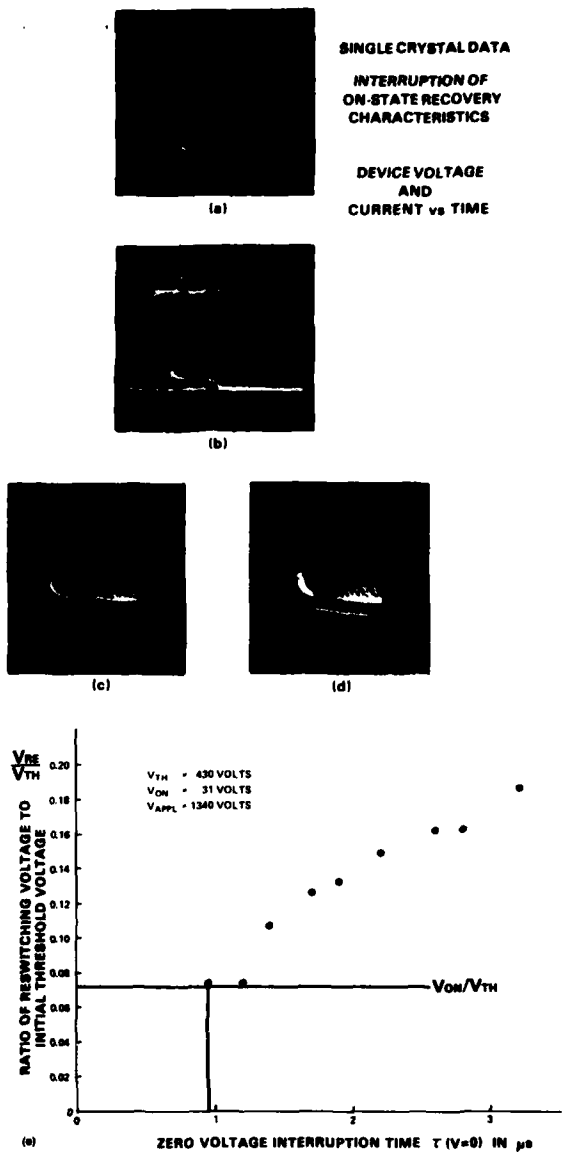

FIG. 2. Interruption studies of the on-state (a) voltage vs time (lower trace) showing set pulse, threshold level switch-on at collapsing voltage, on-state low voltage, and interruption of the on-state for about 150 ns. Note that after the voltage interruption is removed the on-state is recovered without need of reswitching. Scales are 100 V/large division for voltage and 1 μs/large division time. The upper trace gives the current vs time showing ground level, on-current, interruption, and resumption of on-current. (b) Voltage (lower trace at 100 V/div) and current (upper trace) vs time (500 ns /div) showing same effects as in Fig. 2(a). The zero-voltage interruption time is about 600 ns and there is still no signs of reswitching. (c) Voltage (lower trace 20 V/div) vs time (1 μs/div) for eight different interruptions (of on-state) having increasing zero-voltage interruption time indicating the inception of reswitching. This effect is first observed in the oscillogram at $t_{(v=0)} = 1.5\,\mu$s. Switching threshold is off scale. Upper trace shows current vs time for a single interruption. (d) Voltage (20 V/large div) vs time (1 μs/large div) during variable interruptions showing that beginning of reswitching effect occurs at $t_{(v=0)} = 0.85\,\mu$s. Note how the locus of partial recovery curve is traced out on oscillograms 2(c) and 2(d). (e) Plot of actual recovery curve (or ratio of reswitching event to initial threshold voltage vs-voltage interruption time $t_{(v=0)}$ for the single-crystal device of Fig. 2(d). The vertical line is indicative of abscissa intercept for $\tau_{V=0_{max}}$ prior to a measurable reswitching threshold (V_{Re}).

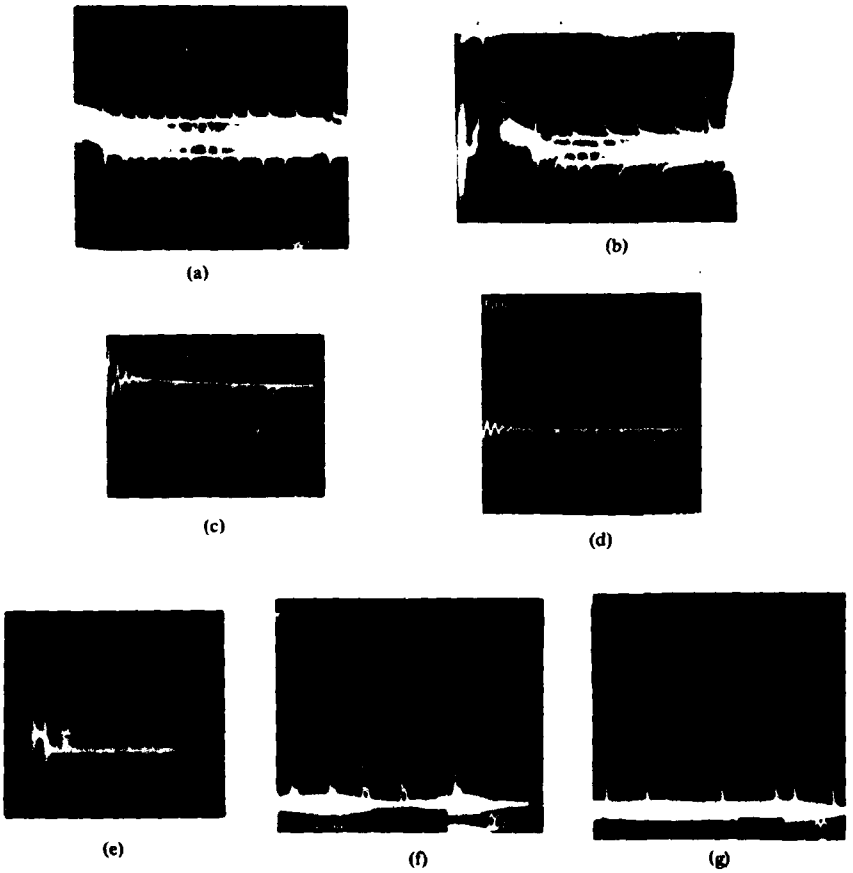

FIG. 3. The recovery of the on-state from single NbO_2 double pulse experiments showing symmetric behavior and very long recovery times. Figures 3(a)–(b) give the voltage waveforms showing the reswitching spikes and the symmetric recovery behavior for positive and negative polarity (10 V/div and 1 μs/div, and 50 V/div and 500 ns/div, respectively). Figure 3(d) shows the consistency of recovered on-current (80 mA/div, 500 ns/div) independent of reswitching threshold. Fig. 3(c) and Figs. 3(e)–3(g) show continued increase in reswitching voltage for increasing zero-voltage interruption time. This suggests very long total recovery times of the order of ms and may repreaent final thermal equilibrium times.

kHz to 1 MHz) studies were conducted by the techniques discussed in Refs. 4 and 5.

III. EXPERIMENTAL RESULTS AND DISCUSSION

A. Recovery phenomena

Interruption type experiments were conducted with the second Cober pulser in Fig. 1(a) synchronized to supply a pulse of equal magnitude to that of the switching pulse, but of the negative polarity, during an interval of the postswitching on-time. The second pulse therefore opposed the set pulse and nulled it out for a specified time. This allows a variable zero-voltage time by changing the width of the second pulse or what is known as the total diagnostic pulse. (A schematic of this type of technique is given in Ref. 8.) Data showing the effect of increasing the zero voltage interruption time on the reswitching properties are given in Figs. 2(a)–2(d). In Figs. 2(c) and 2(d) it is clear that a zero-voltage interruption time ($\tau_{V=0}$) greater than $\tau_2 \simeq 1.4\,\mu$s will cause a significant change in the magnitude of th recovered on-voltage after the interruption pulse is removed. τ_2 has been interpreted as the lifetime of free carriers.[5] The ratio of the reswitching threshold to the initial threshold versus zero-voltage interruption time is plotted in Fig. 2(e) using the recovery curve data from Fig. 2(d).

A different type of experiment, known as a double-pulse study, was performed to determine whether a reversal in polarity could alter the measured value of τ_2 for single-crystal NO_2. In the double-pulse experiment both Cober pulsers have the same polarity, and same magnitude. However, they are separated by a variable interval of interpulse zero voltage. The data shown in Fig. 3 give the increasing threshold magnitude as the interpulse zero-voltage time increases, and indicate that (1) recovery is symmetric for both pulses positive or both negative [Figs. 3(a) and 3(b)]; (2) the recovered on-current is constant as the reswitching voltage is increasing [Figs. 3(c) and 3(d)]; and (3) the recovery process is not entirely complete even after values of $\tau_{(V=0)}$ of several hundred μs. [Fig. 3(g)]. This ultralong final recovery tail is likely to be the thermal equilibrium constant.

B. Current-voltage measurements in the on-state

The voltage and current versus time measurements are given in the oscillograms of Figs. 4(a)–4(c) on a time scale of

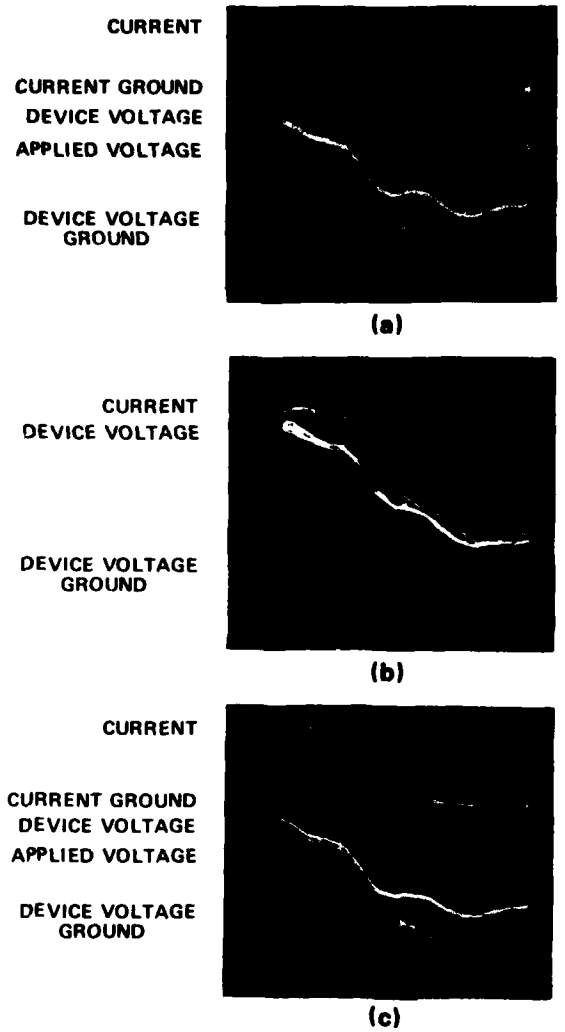

FIG. 4. Oscillograms for a single-crystal NbO_2 device showing current (upper trace 40 mA/div) device voltage (middle trace, 5 V/div), and applied voltage (lower trace, arbitrary scale) vs time (20 ns/div) plus ground lines for current and for device voltage. The trace corresponding to device voltage is broad because it records the superimposed data for five separate on-state interruptions of switching events. Note plateau and irregular features of device voltage as contrasting monotonic behavior of current and applied voltage. The variable parameter in these oscillograms is over-voltage or voltage above minimum threshold for given pulse width: (a) $V_{over} = 670$ V; (b) $V_{over} = 670$ V for broad trace, and $V_{over} = 0$ for the narrow trace above the broad trace (absence of pronounced plateaus); (c) $V_{over} = 870$ V.

20 ns/div. The structure of the voltage-time trace in each oscillogram clearly shows plateau regions in the intervals of 20–40 ns and 70–100 ns into the interruption. These regions correspond to monotonically and smoothly decreasing current (upper trace) and to monotonically and smoothly decreasing *applied* voltage [lower curved trace in Figs. 4(a) and 4(c)]. The device voltage trace is wider than both the current and the applied voltage traces because it consists of five (reproducibly) recorded interruptions of the on-state after switching events, whereas the corresponding applied voltage and current were only recorded (in memory) once. It is interesting to note that the plateau structure of the voltage profile is consistently less pronounced [Fig. 4(b) center trace just above wide voltage trace] when switching is accomplished at minimum threshold conditions ($V_{appl} \simeq V_{th}$), i.e., with essentially zero over-voltage.

The current dependence during the monotonically and smoothly declining applied voltage is plotted against device voltage at the interruption times shown in Fig. 5, as taken from data of Fig. 4(c). The *I-V* characteristics show on the average a linear behavior from 10 to about 60 ns, and a subsequent region of rapidly decreasing current corresponding to a slightly decreasing device voltage (60–100 ns) finally followed by the superlinear and linear low-voltage higher-impedance subregime (100–120 ns). The transitional regime (region IV in Fig. 5) appears to develop when the on-voltage is reduced below the holding voltage for a time in excess of the trap emission time into the valence band, referred to as τ_1. Since the holding voltage in this device is 20–25 V, the critical time period, derived from region IV in Fig. 5 appears to be $\tau_1 = 10$–20 ns. The total time (τ_3) beneath the holding voltage, which is required for the actual development of the lower conductance subregime in the on-state, is about 50–70 ns as shown in Fig. 5 in regions III and IV. The meaning of the holding voltage measurement for *single-crystal* devices will be discussed later.

For polycrystalline devices short interruptions of the on-state obtained by pulses similar to those of Fig. 4 also yielded regions of approximately constant voltage corresponding to decreasing current. The lower-conductance subregime of the on-state is found as in Fig. 5. However, these data were not as clean as the single-crystal data because of the requirement of point contact pressure probes and longer connecting wires to reach the micromanipulator. Nonetheless, the device current was clearly not a linear function of device voltage, and plateau regions were also observed. Substitution of a 100-Ω dummy resistor for the device yielded the linear dependence of current on voltage expected from a material devoid of traps.

Some polycrystalline devices displayed a sufficiently low threshold voltage that the on-state could be maintained dynamically with a postswitching subthreshold sine, triangular, or square wave as in Ref. 5. The details of the cw experiments are given in Ref. 8. The holding voltage, for such a device, as determined by a curve tracer [Fig. 6(a)], was 3.4 V. The holding voltage V_h is defined as the minimum on-state voltage in the down-voltage direction prior to the development of current-controlled negative differential resistance. The latter negative region is interpreted to represent the inception of the switch-off transition mechanism. The time until the development of the lower-conductance subregime can be extracted from cw oscillogram data in Figs. 6(b) or 6(c) as the time between $V = V_h$ and the change is slope of the current vs time trace. This current I_k corresponds to the knee voltage V_k. This time interval derived from the cw data of Fig. 6(c), is about 270 ns. Single-crystal data of Fig. 5 yields 40–50 ns for the comparable interval. The corresponding time interval from the previous polycrystalline study of devices having aluminum contacts is about

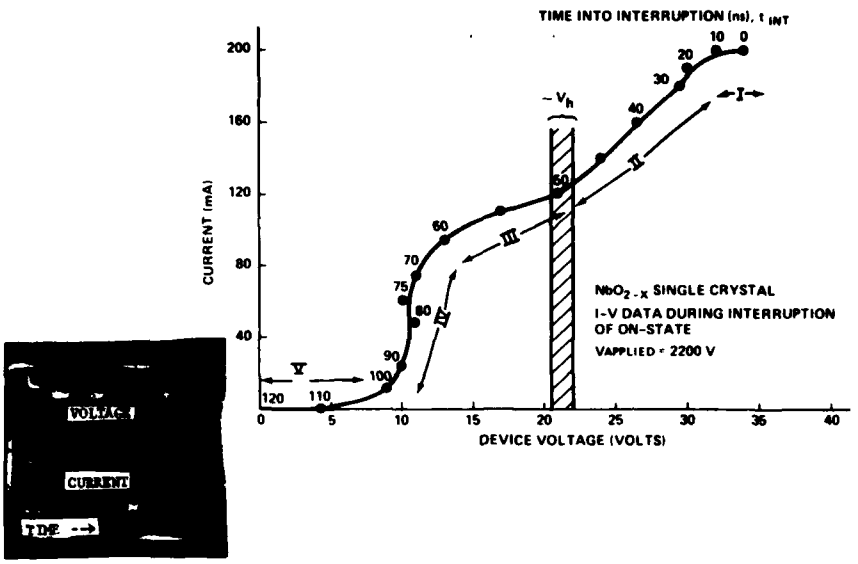

FIG. 5. On-state I-V characteristic for NbO_2 single-crystal device. Plot of current vs device voltage during interruption of on-state using data of Fig. 4(c). Data are plotted in a point-by-point manner as a function of time to show sharp decrease in current at conditions where voltage is less than the holding value ($V_h = 22$ V at $t_{int} = 50$ ns) for about 20 ns. This is interpreted as a transitional regime of relatively constant voltage (plateau) from the conduction band to a trapping band (region IV). Inset shows expanded scale of voltage plateau region corresponding to decreasing current for an interruption of a different switching event. ($t = 4$ ns/div).

100 ns.[4,5] Figure 7 gives the holding votlage for single-crystal NbO_2 from curve tracer data, and shows that the switch-off for single-crystal devices occurs from the lower conductance subregime of the on-state without observed discontinuity in the 120-Hz data.

C. Character of the current during interruption of the on-state

The character of the current during the decreasing voltage excursion will be discussed according to Fig. 5 where we distinguished five different regions of behavior.

Region I (0–10 ns): The first part of this region is probably related to the free-carrier response time which is limited by the dielectric relaxation time $\tau_d = RC = (35\ V/0.2\ A)(5\times 10)^{-12}$ pF) $= 10^{-9}$ sec. Thus a ns probably occurs before the voltage is actually visible. During the region 1–10 ns the current shows little or no decay, probably because the trap release time is of the order 10 ns.

Region II (10–50 ns, $R = 125\,\Omega$): This interval displays linear characteristics and thus appears to represent the true I-V characteristics of the metal-like on-state of NbO_2. The region from 20 to 30 ns corresponds to the first plateau region in the V vs t data in Figs. 4(a)–(c). Microscopically it may represent the beginning of a conduction band emptying into unoccupied shallow donor states. Region II is approximately extrapolatable through the origin.

Region III (50–60 ns, $R = 330\,\Omega$): This region, located at voltages under the holding value, may be associated with the start of a relaxation to the transitional state.

Region IV (70–90 ns, $R = 20\,\Omega$): This is clearly the transitional region from the high-current metal-like regime to the lower-conductance subregime. It corresponds to the second-plateau region in Fig. 4(c). This plateau region is far more pronounced at higher over-voltage than at the zero-over-voltage event shown in Fig. 4(b). There is no change in the plateau structure as the applied votlage is increased from 1330 to 2200 V, that is, a range of almost 900 V in over-voltage has no apparent effect on the knee structure of the transitional regime (region IV). Thus we assume that traps are saturated just above the threshold, and that the knee structure is indicative of trap emptying.

At high over-voltage the bands are more populated with free carriers, and are apparently more perturbed overlapping, and/or interacting. We interpret the transitional regime to be caused by a voltage that is less than the holding value for a time in excess of the trap emission time. This is supported in Ref. 5, wherein no such regime occurs for rapid descent of on-voltage as accomplished by a 1-MHz square wave.

At low-frequency (120 Hz), single-crystal devices of NbO_2 do not show the same type of on-state I-V behavior as the voltage is decreased as do the polycrystalline devices. The latter, as seen in Fig. 6(a), displays the presence of a pronounced negative region and of a switch-off transient. The single-crsytal curve tracer data of Fig. 7 has a voltage at the knee condition corresponding consistently to the voltage for the inflection point between regions II and III (at 50 ns into the interruption in Fig. 5). This may add credence to the suggestion that the increased differential resistance of region III relative to that of region II may be due to falling beneath the holding voltage and consequent decay of some carriers.

Region V (100–120 ns, $R = 750\,\Omega$): The I-V regime of region V is referred to herein as the lower conductance sub-

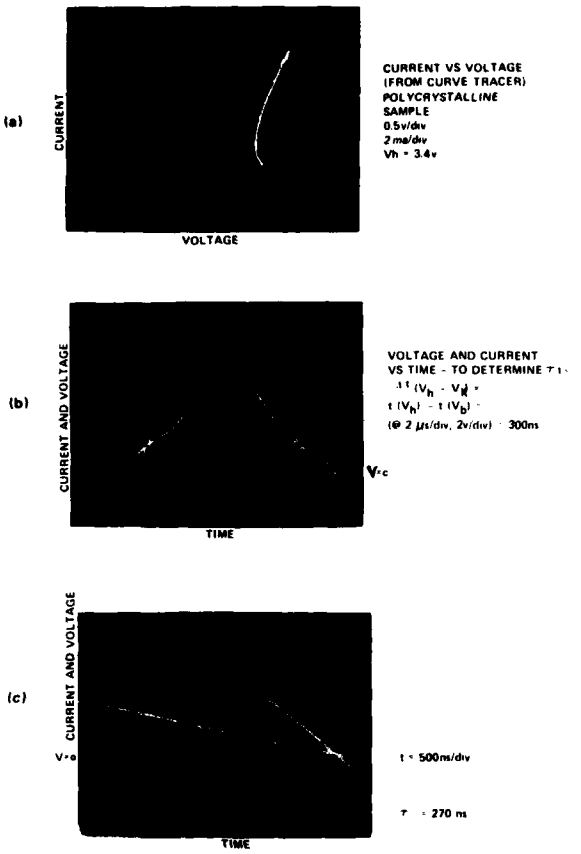

FIG. 6. On-state data for polycrystalline devices showing holding voltage (V_h) and knee current (I_k). (a) (Current 2 ma/div) vs voltage (0.5 V/div) taken on curve tracer (120 Hz). The data shows the on-state (upper curve) for decreasing voltage passing through minimum device voltage followed by negative resistance region and switch-off transient to off-state. From this data V_h is taken as 3.4 V for the polycrystalline NbO_2 device. (b) Voltage (upper trace 2 V/div) and current (showing knee) vs time (2 μs/div) for on-state sustained by 152 kHz triangular wave. From these data we estimate the time between V_h and V_k as $\sim$ 300 ns, where V_k is the voltage at the knee in current I_k. (c) Same as Fig. 7(b) except t = 500 ns/div, hence we estimate $t_{(V_h)} - t_{(I_k)} = 270\ \text{ns} \simeq \tau_3$. This is the time below the holding voltage for the development of the blocked state or what is presently interpreted as approximating the distribution trapped carrier decay time τ_1 for the polycrystalline device.

regime of the on-state. In the present interpretation this region could correspond to hopping conduction in a trapping level or band. Such a band can only accept free carriers from the conduction band after the trapped carriers emission time (τ_1 = 10–20 ns) has been exceeded. This means that the carriers which were trapped during the preswitching regime have had enough time to decay in order to leave trapping sites vacant for the capture and recombination of carriers which were in the conduction band during the Ohmic region II and III. The manner in which a trapping can arise from a crystal chemical standpoint in nonstoichiometric NbO_2 is described in the Appendix to this paper. Alternatively, region V may be associated with residual trapped charge and consequent high-resistance regions near the contacts, provided there exists an asymmetry in charge distribution.

IV. CONCLUSIONS

From the above discussion and data it is clear that there are two time constants regulating the behavior of the on-state characteristics of NbO_2. The shorter of these time constants, τ_1, which we estimate at about 10–20 ns, seems to be associated with localized trapped carriers whose recombination back into valence states lead to transitional regime. The longer time constant τ_2 (about 0.8–1.2 μs), seems to be associated with the decay of the free-carrier concentration such that a reswitching event is necessitated.

The ratio of these time constants τ_1/τ_2 should yield an indication of the proportion of free carriers which, when recombined, will trigger avalanched recombination into the trapped band and ultimately into the valence band. Thus (10–20 ns/0.8–1.2 μs = 1/60th of 5×10^9 recombinations, or about 10^8 recombinations appear to trigger the instability which generates the tranistional regime. Such a recombination could be ample to remove any screening effects and generate the reverse of a postulated insulator-metal Mott transition. It should also be noted that the ratio of the differential resistance of region IV to that of region V is approximately 20 Ω /750 Ω or about 1:40, corresponding to changes in carrier concentration and mobility. This agrees with the relationship that $\tau_2/\tau_1 \simeq G_2/G_1$, where G_2 refers to the conductance of the transitional regime and G_1 to the lower conductance regime. This supports the contention that the lower conductance subregime is governed by the carrier associated with τ_1. In the lower-conductance regime the recombined centers could participate in hopping conduction. However, the transitional regime is probably influenced strongly by free carriers as well as by trapped carriers.

Finally we should note that single-crystal devices and polycrystalline devices seem to indicate differences in their comparative τ_1 and τ_2 values. Recalling that τ_3 refers to the total time beneath the holding voltage prior to the develop-

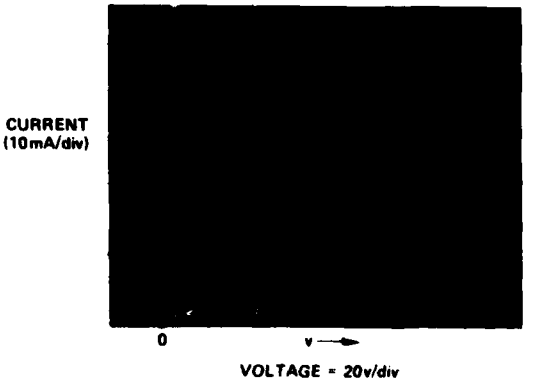

FIG. 7. Current (10 mA/div) vs voltage (20 V/div) at switching and in down-voltage direction for a *single crystal* device taken on curve tracer, showing off-state and switch-on threshold (horizontal trace) and on-state for decreasing voltage (vertical trace). This shows a knee at V = 22 V assumed to represent V_h. Note absence of switch-off transient during on-state regime, in contrast to Fig. 6(a). This observation has been an important and consistent distinction between single-crystal and polycrystalline NbO_2 threshold switching devices. Arrowhead shows direction of increasing time from zero to positive phase.

ment of the lower conductance regime, we note that the data from Figs. 5 and 6 show τ_3 (single)/ τ_3(poly) = 50 ns/270 ns. This suggests a far longer trap release time (τ_1) or a stronger trapping probability for polycrystalline NbO_2. This is entirely reasonable from a defect oxide standpoint, the polycrystalline structure supplying a far greater diversity of trapping mechanisms. The data also indicate that τ_2 (single)/τ_2 (poly) = $\sim 1\,\mu$s/200 ns, which is interpreted to mean that for an equal field there are apparently more free carriers in the conduction band of a single-crystal device than for a polycrystalline counterpart. This also is reasonable from the standpoint of more perfect materials promoting delocalization of charge, longer mean free paths and times, and higher free-carrier concentrations.

APPENDIX

The change in current during the transitional regime from 60 to 100 ns (in Fig. 5) into the interruption is about 83 mA, or $\Delta I/\Delta t = -83\times10^{-3}\,\text{A}/40\times10^{-9}\text{s} \approx -2\times10^{6}$ A/s or -2×10^{6} (Coul/sec^2). The rate of voltage change during this interval is $-4\,\text{V}/40\times10^{-9}\,\text{s} = -1\times10^{+8}$ V/s. Dividing tells us that for every volt decrement in onpotential there will occur 1×10^{17} electron/sec decay or in an inverval of 40 ns in which the voltage is decreased by 4 V(the transitional regime in Fig. 5), there will occur $4\times10^{17}\times40\times10^{-9} \approx 1.6\times10^{10}$ electron recombinations. We now assume that these recombinations are accomplished through trapping sites furnished by the niobium ions which compensate for the oxide nonstoichiometry. From a crystal chemistry standpoint we can write the nonstoichiometric form of NbO_2 as NbO_{2-x} and retain charge balance by assuming some fraction of cations to be in a lower oxidation state than +4.

Thus we rewrite NbO_2 as

$$[(Nb_y^{4+})(Nb_{1-y}^{2+})]O_{2-x}^{2-}.$$

We know from previous work that the nonstoichiometric compound $NbO_{1.87}$ represents the lowest oxygen content for reproducible threshold switching of polycrystalline devices. Therefore if we take $x = 0.13$ and solve the charge balance equation, we arrive at $y = 0.87$.

This suggests that at $y = 0.87$ there will exist too many NbO_2 trapping centers in order that trap saturation or near saturation could be accomplished by the electric field. Assuming no other trapping mechanism this implies that the ratio of Nb^{+4} to Nb^{+2} must be greater than $0.87/0.13 \approx 6{:}1$.

[1] G. K. Gaulé, P. La Plante, S. Levy, and S. Schneider, IEDM Tech Digest, Ft. Monmouth, New Jersey, p. 274 (unpublished).
[2] L. M. Levinson, H. R. Phillip, and G. A. Slack, ECOM Research and Development Rep. 76-1331-F, 1976 (unpublished).
[3] S. H. Shin, T. Halpern, and P. Raccah, J. Appl. Phys. **48**, 3150 (1977); and S. H. Shin and P. M. Raccah, Bull. Am. Phys. Soc. **21**, 302 (1976).
[4] G. C. Vezzoli, J. Appl. Phys. **50**, 6390 (1979).
[5] G. C. Vezzoli, Phys. Rev. **19**, 6469 (1979).
[6] B. Lalevic, M. Shoga, M. Gvishi, and S. Levy (unpublished).
[7] B. Lalevic (unpublished).
[8] G. C. Vezzoli, L. W. Doremus, and P. J. Walsh, J. Non Crystall. Solids **18**, 333 (1975); also see G. C. Vezzoli, J. Appl. Phys. **50**, 5810 (1979); Appl. Phys. Lett. **35**, 288 (1979).
[9] P. Walsh and G. C. Vezzoli, Appl. Phys. Lett. **25**, 28 (1974).

Unclassified

SECURITY CLASSIFICATION OF THIS PAGE (When Data Entered)

REPORT DOCUMENTATION PAGE

READ INSTRUCTIONS BEFORE COMPLETING FORM

1. REPORT NUMBER: 13978.6-P	2. GOVT ACCESSION NO.: AD-A106136 N/A
3. RECIPIENT'S CATALOG NUMBER: N/A	
4. TITLE (and Subtitle): The On-State of Single-Crystal and Polycrystalline $LiNbO_3$	5. TYPE OF REPORT & PERIOD COVERED: Reprint
	6. PERFORMING ORG. REPORT NUMBER: N/A
7. AUTHOR(s): Gary C. Vezzoli, G. K. Gaule, L. W. Doremus, B. Lelevic, Steve Levy, M. Shoga	8. CONTRACT OR GRANT NUMBER(s): DAAG29-80-C-0072
9. PERFORMING ORGANIZATION NAME AND ADDRESS: Rutgers University, Piscataway, NJ 08854	10. PROGRAM ELEMENT, PROJECT, TASK AREA & WORK UNIT NUMBERS: N/A
11. CONTROLLING OFFICE NAME AND ADDRESS: U. S. Army Research Office, P. O. Box 12211, Research Triangle Park, NC 27709	12. REPORT DATE: Feb 81 13. NUMBER OF PAGES: 7
14. MONITORING AGENCY NAME & ADDRESS (if different from Controlling Office)	15. SECURITY CLASS. (of this report): Unclassified 15a. DECLASSIFICATION/DOWNGRADING SCHEDULE

16. DISTRIBUTION STATEMENT (of this Report)

Submitted for announcement only.

17. DISTRIBUTION STATEMENT (of the abstract entered in Block 20, if different from Report)

18. SUPPLEMENTARY NOTES

19. KEY WORDS (Continue on reverse side if necessary and identify by block number)

20. ABSTRACT (Continue on reverse side if necessary and identify by block number)

407650

DD FORM 1 JAN 73 1473 EDITION OF 1 NOV 65 IS OBSOLETE

Unclassified

SECURITY CLASSIFICATION OF THIS PAGE (When Data Entered)